

Tuning the Properties of Photonic Films from Polymer Beads by Chemistry

Marc Egen and Rudolf Zentel*

Institute of Organic Chemistry, Johannes Gutenberg-University, Duesbergweg 10-14, D-55099 Mainz, Germany

Received October 24, 2001. Revised Manuscript Received February 7, 2002

This paper describes the preparation of monodisperse colloids from various methacrylates. These colloids sediment well on glass slides and form—in the dried state—large three-dimensional face-centered cubic photonic crystal films with Bragg reflection in the visible region. Depending on crystallization conditions, the domain sizes vary between 50 and 300 μm . By cross-linking the polymer within the colloids, it is possible to increase the thermal stability of the polymeric photonic structure tremendously (up to 1 h at 200 °C). These photonic structures soften above T_g (rubbery photonic structure), but they cannot fuse. Cross-linked colloids from poly(*tert*-butyl methacrylate) can either thermally or chemically be modified. During thermal treatment (above 200 °C) the colloids shrink, as isobutene is split off. This allows a change of the lattice constant and the reflection color of an already crystallized dry photonic film. The acid-catalyzed cleavage of the ester bond allows the conversion of existing photonic structures into photonic crystals from core–shell colloids with hydrophilic polyelectrolytes in the shell.

Introduction

Photonic band gap materials have been of great interest since Yablonovitch¹ and John² introduced the idea of confinement and control of light and its emission by a photonic crystal. Photonic properties can be achieved in one, two, or three dimensions by changing the refractive index periodically. Light confinement in one direction can be achieved with a layered arrangement of different refractive index materials. Two-dimensional arrays are realized with help of photolithographic techniques, for example, by arranging cylinders from high refractive material in a hexagonal order or by drilling holes into a material.³

To build up three-dimensional photonic crystals, there are basically two concepts. The first uses techniques known from the processing of semiconductors. Three-dimensional structures prepared in this way allow—so far—only the manipulation of IR radiation (patterning in the micrometer region or slightly below). Yablonovitch followed this concept and introduced the so-called “yablonovites”, for which a material is perforated with cylinders.⁴ The drilling angle is chosen to give an fcc-comparable structure within a high refractive index material. Another approach is the so-called “woodpile” structure that is formed via wafer-fusion and laser-beam-assisted alignment techniques. A complete photonic band gap for the near-infrared wavelength was reported recently for a woodpile structure formed from silicon.^{5,6}

A second approach uses the self-assembly of nanometer-sized particles.⁷ In this case three-dimensional

photonic crystals are formed by the crystallization of colloids. If they are monodisperse in their diameter, they form usually a cubic closest packed crystal that is quoted as an artificial opal. Artificial opals reflect visible light. They are made either from silica (the classical case)⁸ or from polymers such as polystyrene⁹ or other hydrocarbon-backbone polymers¹⁰ (polymer opals). Generally, polymer opals offer a larger chemical variability to adjust the refractive index, to perform surface chemistry, or to incorporate fluorescent dyes compared to silica opals. Recently, we could prepare large opaline films from poly(methyl methacrylate) (PMMA) colloids.^{11,12} The voids within all these opaline materials can be filled with an inorganic high refractive index material. By removal of the original opaline material (e.g., dissolution of the polymer), inverted opals can be prepared.^{13–15}

To optimize the optical properties of a three-dimensional photonic band gap material, the material should possess a high refractive index to achieve a high

(1) Yablonovitch, E. *Phys. Rev. Lett.* **1987**, *58*, 2059.
 (2) John, S. *Phys. Rev. Lett.* **1987**, *58*, 2486.
 (3) Li, A. P.; Müller, F.; Birner, A.; Nielsch, K.; Gösele, U. *J. Appl. Phys.* **1998**, *84*, 6023.

(4) Yablonovitch, E. *J. Mod. Opt.* **1994**, *41*, 173.
 (5) Lin, S. Y.; Fleming, J. G.; Hetherington, D. L.; Smith, B. K.; Biswas, R.; Ho, K. M.; Sigalas, M. M.; Zubrzycki, W.; Kurtz, S. R.; Bur, J. *Nature* **1998**, *394*, 251.
 (6) Noda, S.; Tomoda, K.; Yamamoto, N.; Chutinan, A. *Science* **2000**, *289*, 604.
 (7) Xia, Y.; Gates, B.; Li, Z.-Y. *Adv. Mater.* **2001**, *13*, 409.
 (8) Stöber, W.; Fink, A.; Bohn, E. *J. Colloid Interface Sci.* **1968**, *26*, 62.
 (9) Goodwin, J. W.; Hearn, J.; Ho, C. C.; Ottewill, R. H. *Colloid Polym. Sci.* **1974**, *252*, 464.
 (10) Xia, Y.; Gates, B.; Yin, Y.; Lu, Y. *Adv. Mater.* **2000**, *12*, 693.
 (11) Müller, M.; Zentel, R.; Maka, T.; Romanov, S. G.; Sotomayor-Torres, C. M. *Chem. Mater.* **2000**, *12*, 2508.
 (12) Müller, M.; Zentel, R.; Maka, T.; Romanov, S. G.; Sotomayor-Torres, C. M. *Polym. Prepr. (Am. Chem. Soc., Div. Polym. Chem.)* **2000**, *41*, 810.
 (13) Vlasov, Y. A.; Luterova, K.; Pelant, I.; Hönerlage, B.; Astratov, V. N. *Appl. Phys. Lett.* **1998**, *71*, 1616.
 (14) Blanco, A.; Lopez, C.; Mayoral, R.; Miguez, H.; Meseguer, F.; Mifsud, A.; Herrero, J. *Appl. Phys. Lett.* **1998**, *73*, 1781.
 (15) Romanov, S. G.; Johnson, N. P.; Yates, H. M.; Pemble, M. E.; Butko, V. Y.; Sotomayor-Torres, C. M. *Appl. Phys. Lett.* **1997**, *70*, 2091.

refractive index contrast ($n_1/n_2 \approx 2.8$). In addition to that, inverted opaline structures (replica) exhibit a broader band gap.¹⁶ Replicas from dried colloidal crystals that consist of high refractive inorganic materials come close to these requirements. Little chemistry has, however, so far been done to optimize "polymer opals" for replica preparation. Usually, the preparation of inorganic replica is made by sol-gel chemistry. To provide suitable and designed systems for this process, the modification of the surface polarity of the beads can be essential. Therefore, polymer beads from polymethacrylates become interesting, as they allow chemistry at the surface.

Infilling by sol-gel chemistry has also a drawback. Because of the evaporation of solvent during the infilling process, several structural defects appear such as incomplete crystallization or nanoporous holes. Both reduce the filling factor and decrease the effective refractive index.

Preventing these obstacles leads to infilling via gas-phase reactions. In this context thermal stability of the polymer beads becomes a limiting factor, as it allows so far only the use of lower boiling inorganics such as SnCl_4 .¹⁷ Colloidal crystals prepared from cross-linked polymethacrylates can be an advantage for this purpose.

In a more general way, monodisperse beads from ester-functionalized polymers open ways to chemical reactions such as ester cleavage or substitution of ester side chains in the colloidal crystal. With chemical modification it is also possible to modify only the outer part of colloidal spheres to generate core-shell systems. Core-shell systems represent interesting structures with preparative and theoretical research relevance. Topics such as electrostatic interactions between highly charged colloids, polyelectrolytes on surfaces, and chemical modifications in already structured arrays of monodisperse spheres are exciting and interesting fields of colloidal research.¹⁸⁻²⁶

The aim of this work is (1) to broaden the chemical basis for "polymer opals", (2) to increase the thermal stability of polymer opals, and (3) to modify the surface of the polymer beads within polymer opals.

Results and Discussion

Colloidal spheres of different sizes varying from 200- to 350-nm diameters were synthesized via surfactant-free emulsion polymerization. Mainly the polymerization of two monomers was investigated. Methyl methacrylate (MMA), for which we had shown¹¹ the possibility

Table 1. Reaction Conditions for the Preparation of Monodisperse Colloids

colloids ^a	vol. H_2O (mL)	monomer (mL)	toluene (mL)	reaction time (min)	λ_{Max} (nm)	d^b (nm)
C-MMA-1	130.0	15.0	15.0	45.0	643	289
C-MMA-2	5.6	0.6	0.6	>800	>360 ^c	
C-MMA/Et(1)	6.0	0.6	0.6	16.0	519	233
C-MMA/Et(2.5)	6.0	0.6	0.6	12.0	506	227
C-MMA/Et(5)-1	140.0	15.0	15.0	13.0	580	261
C-MMA/Et(5)-2	6.0	0.6	0.6	10.0	538	242
C-MMA/Et(5)-3	6.0	0.6	0.6	8.5	576	259
C-MMA/Et(10)	6.0	0.6	0.6	7.0	570	256
C-tBMA-1	140.0	15.0	15.0	60.0		^d
C-tBMA-2	5.0	0.6	0.6	32.0		^d
C-tBMA-3	165.0	15.0	<i>e</i>	24.0	542	247
C-tBMA-4	6.6	0.6	<i>e</i>	8.5	570	260
C-tBMA-5	6.6	0.6	<i>e</i>	9.0	760	346
C-tBMA/Et(5)	6.0	0.6	<i>e</i>	7.5	570	260

^a Sample name (MMA = colloids from methyl methacrylate, tBMA = colloids from *tert*-butyl methacrylate, Et(*x*) = colloids cross-linked with *x* mol % ethylene glycol bis methacrylate). ^b Colloid diameter calculated from eq 1. ^c Colloid diameter out of the measuring range, polydisperse colloids. ^d Precipitating solid instead of colloids. ^e Reaction performed without toluene.

to prepare large photonic films, was used to optimize processes such as crystallization and thermal treatment. *tert*-Butyl methacrylate (tBMA) was used because it allows easy chemical modification by splitting off isobutene. In Table 1 the reaction conditions as well as properties of the resulting photonic structures are summarized. The polymerization was optimized for two reaction vessels, a large and a small one. As a result, highly monodisperse polymer lattices were obtained, which show Bragg reflection from cast films. Although we did not characterize the standard deviation of the diameters of colloids, they must be better than 5%²⁷ as judged from the quality of the colloidal crystals to be discussed later.

For the polymerization of MMA we had added some toluene to improve stirring conditions. This did not work well for the polymerization of tBMA (see **C-tBMA-1 + 2** in Table 1). Therefore, the colloids from poly(*tert*-butyl methacrylate) (PtBMA) were prepared without toluene. Treating the reaction mixture with air for at least 5 min stopped the polymerization. After the evaporation of toluene and remaining monomer, the suspension was filtered through a standard paper filter. Thereby large agglomerations of polymer were separated. A centrifugation was following to exempt the obtained suspension from remaining agglomerations and low molecular impurities (see Experimental Section). After four to five centrifugation cycles, the polymer lattices were stored in water at concentrations of 10 to 30 wt %.

The size of beads can be adjusted by reaction time. Because initiator concentration and diffusion rate of monomer from the large monomer droplets into the polymer containing micelles keeps constant during polymerization, the micelles grow in cubic root dependence as a function of time. Figure 1 shows this behavior for colloids made from tBMA (**C-tBMA-3**).

To prepare a film from self-assembled colloids, several microliters of a polymer suspension was spread on a hydrophilized glass substrate. Careful drying in a

- (16) Busch, K.; John, S. *Phys. Rev. E* **1998**, *58*, 3896.
- (17) Müller, M.; Zentel, R.; Maka, T.; Romanov, S. G.; Sotomayor-Torres, C. M. *Adv. Mater.* **2000**, *12*, 1499.
- (18) Caruso, F. *Adv. Mater.* **2001**, *13*, 11.
- (19) Wang, D.; Caruso, R. A.; Caruso, F. *Chem. Mater.* **2001**, *13*, 364.
- (20) Hotz, J.; Meier, W. *Langmuir* **1998**, *14*, 1031.
- (21) Rogach, A.; Susha, A.; Caruso, F.; Sukhurov, G.; Kornowski, A.; Kershaw, S.; Möhwald, H.; Eychmüller, A.; Weller, H. *Adv. Mater.* **2000**, *12*, 333.
- (22) Guo, X.; Weiss, A.; Ballauf, M. *Macromolecules* **1999**, *32*, 6043.
- (23) Müller, H.; Nuyken, O.; Strohriegel, P. *Makromol. Chem., Rapid Commun.* **1992**, *13*, 125.
- (24) Holtz, H.; Asher, S. A. *Nature* **1997**, *389*, 829.
- (25) van Blaaderen, A.; Vrij, A. *J. Colloid Interface Sci.* **1993**, *156*, 1.
- (26) Thurmond, K. B., II.; Kowalewski, T.; Wooley, K. L. *J. Am. Chem. Soc.* **1997**, *119*, 6656.

- (27) Cheng, B.; Ni, P.; Jin, C.; Li, Z.; Zhang, D.; Dong, P.; Guo, X. *Opt. Commun.* **1999**, *170*, 41.

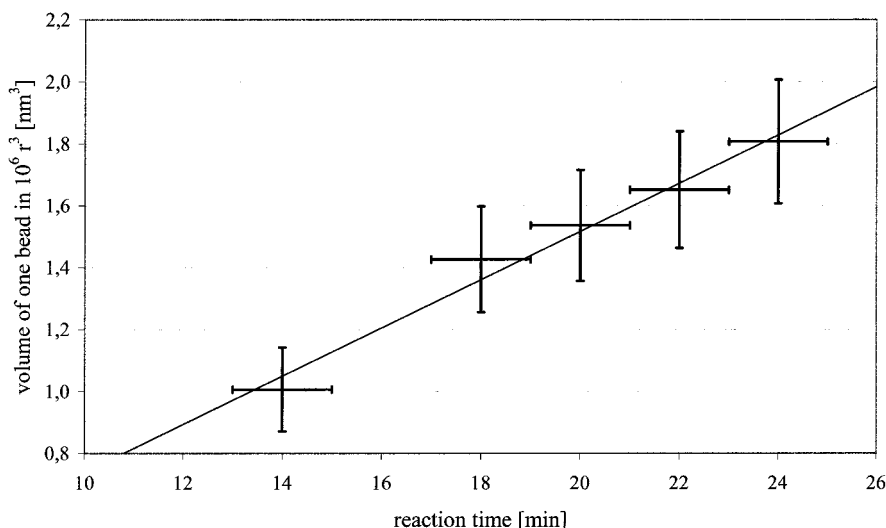


Figure 1. Time-dependent growth of colloids of **C-tBMA-3**. Time dependence of the volume of one bead of **C-tBMA-3** during ongoing polymerization. Volumes were calculated with λ_{111} and eq 1. Error bars are calculated via half bandwidths

chamber with high relative humidity leads to crystallization and the formation of an uniform, iridescent film extending over several square centimeters (see Figure 2a). Microscopic observation shows that this iridescent film is homogeneous at first. However, during the final drying stage vertical cracks appear in the crystal (see Figures 2b and 6). The resulting domains range from the $10\text{-}\mu\text{m}$ regime for samples dried for several hours up to $300\text{ }\mu\text{m}$ for samples dried very slowly (several days) at high relative humidity conditions (Figure 2b). All domains reflect the same color (wavelength of light). This proves that in all cases their 111 plane is oriented parallel to the substrate. More details can be obtained by a careful inspection of domains of photonic crystals from larger beads (see, for example, Figure 2b). Thin lines, which are probably height steps (see also Figure 5) cross the cracks undisturbed. This means that orientational order between the domains is not lost during shrinkage and crack formation. We have indications that domains in the millimeter regime are possible by drying on liquid substrates. These investigations will be published elsewhere.

Polymer opals from spheres with sizes mentioned above exhibit a characteristic peak in the visible regime of the electromagnetic radiation. This peak is related to the Bragg diffraction of the 111 plane in the fcc arrangement of colloidal spheres. For quantitative characterization, UV-transmission spectra were recorded with a beam size of 2 mm^2 (Figure 3). Thus, the beam size averages over many domains. The sharpness of the "virtual absorption" (reflection) requires the 111 planes in all domains to be parallel to each other. This supports the microscope observations.

Figure 3 shows also peaks of higher order in addition to the 111 peak. This proves the quality of the packing. These peaks are found in the visible regime if the reflection is in the near-IR regime (larger beads). From calculations the full photonic band gap is expected to occur for higher order reflections.²⁸ The opaline films from larger beads are therefore an interesting starting material for the preparation of inorganic replica, which might show a full photonic band gap.¹⁷

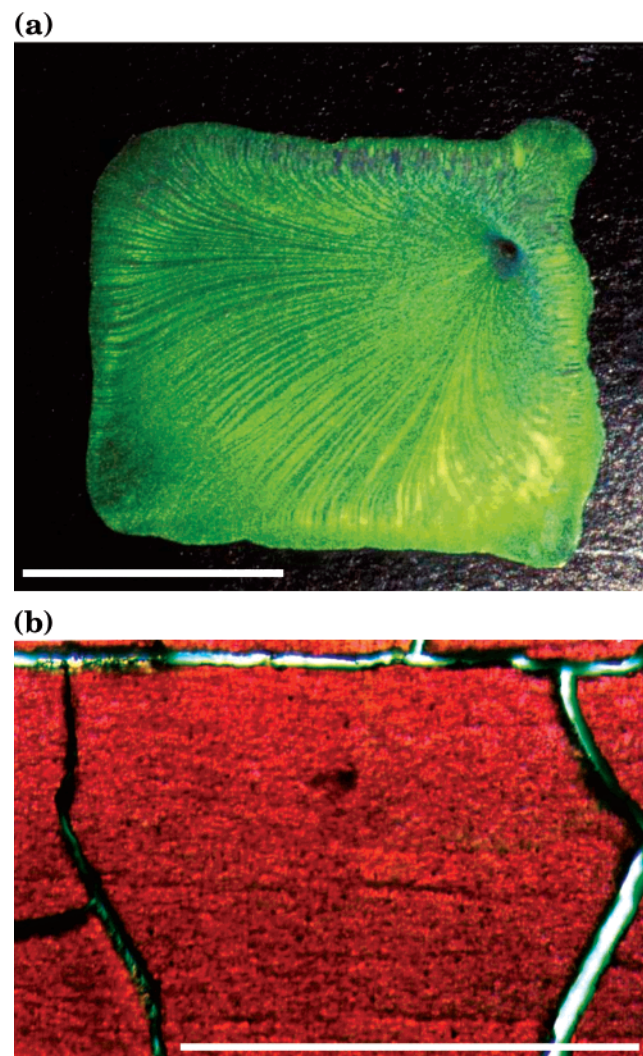


Figure 2. (a) Photograph of a photonic film from **C-tBMA-3**; length of bar equals 1 cm. (b) Microscope image of a photonic film from **C-tBMA/Et(5)-1** with transmitted illumination; length of bar equals $250\text{ }\mu\text{m}$.

The diameters of spheres are related to the reflected wavelength (perpendicular incidence) by a modified

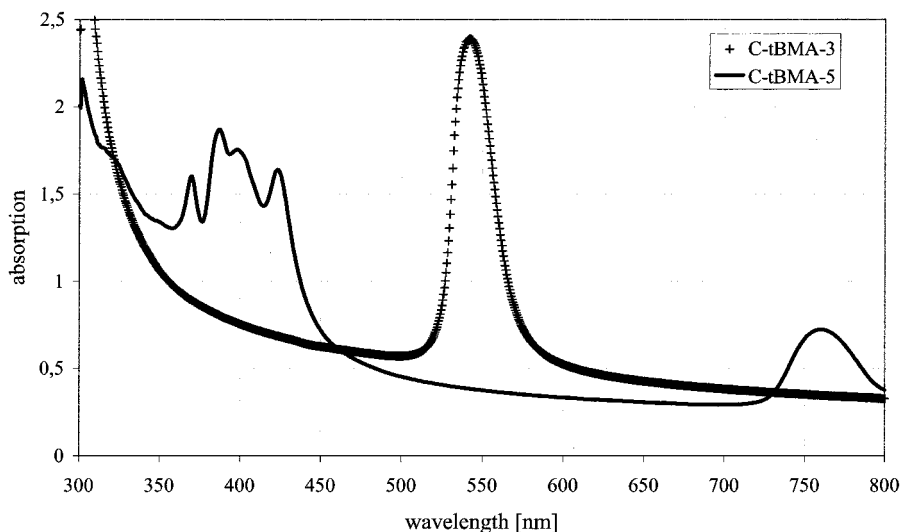


Figure 3. Selected UV-vis spectra of different photonic films with λ_{Max} at 760 nm (C-tBMA-5) and 542 nm (C-tBMA-3). Note the higher order reflections from 350 to 450 nm for (C-tBMA-5).

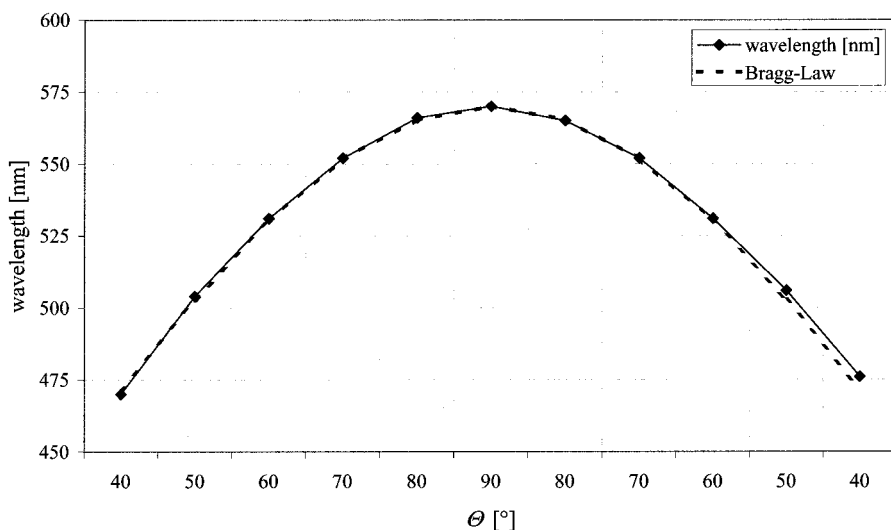


Figure 4. Angular-dependent UV maxima for C-tBMA-4. Θ is the angle between incoming light and the film plane ($\Theta = 90^\circ$: perpendicular to the film).

Bragg law (eq 1).²⁹

$$\frac{\sqrt{3}\lambda_{(111)}}{2\sqrt{2}\sqrt{n_{\text{eff}}^2 - \cos^2 \Theta}} = d \quad (1)$$

Θ is the angle of incidence to the 111 plane. n_{eff} is the effective refractive index calculated with the refractive index of the polymer (PMMA: $n = 1.492$)³⁰ and air ($n = 1.0$) respectively and the filling factor for an fcc packing. The calculation of bead diameters via eq 1 is consistent with SEM measurements.¹¹ The results are compiled in Table 1.

To quantify the color changes at different viewing angles, we measured the UV-vis reflection angular dependent. Figure 4 shows the relation between the incident angle (90° C equals perpendicular incidence of light to the substrate) and the observed wavelength that

is consistent with eq 1. From these data and from the SEM measurements (Figure 5) we conclude that the crystal arrays of fcc-packed beads are homogeneous.

SEM measurements (Figure 5) show large terraces of polymer beads with perfect “hexagonal-like” structure. Especially interesting are the cracks (left side of Figure 5) as they allow a view into the third dimension. The cracks show that the ordered arrangement extends into the bulk of the material.

Thermal Stability of the Photonic Structure

The thermally induced transitions of the colloidal arrays were investigated to correlate the glass transition temperatures (T_g) and the fusing temperature (T_f) at which the photonic structure is irreversibly lost. The results are compiled in Table 2. For this purpose the optical properties of colloidal films were observed in an optical microscope. A glass slide with a film was put into a hotstage and heated at a rate of $4^\circ\text{C}/\text{min}$. While raising the temperature, several effects occur in the colloidal crystal. At about 100°C , existing cracks enlarge. This effect is most probably caused by the

(29) Luck, W.; Klier, M.; Wesslau, H. *Ber. Bunsen-Ges. Phys. Chem.* **1963**, *67*, 75–84.

(30) *Polymer Handbook*, 3rd edition; Wiley-Interscience: New York, 1998.

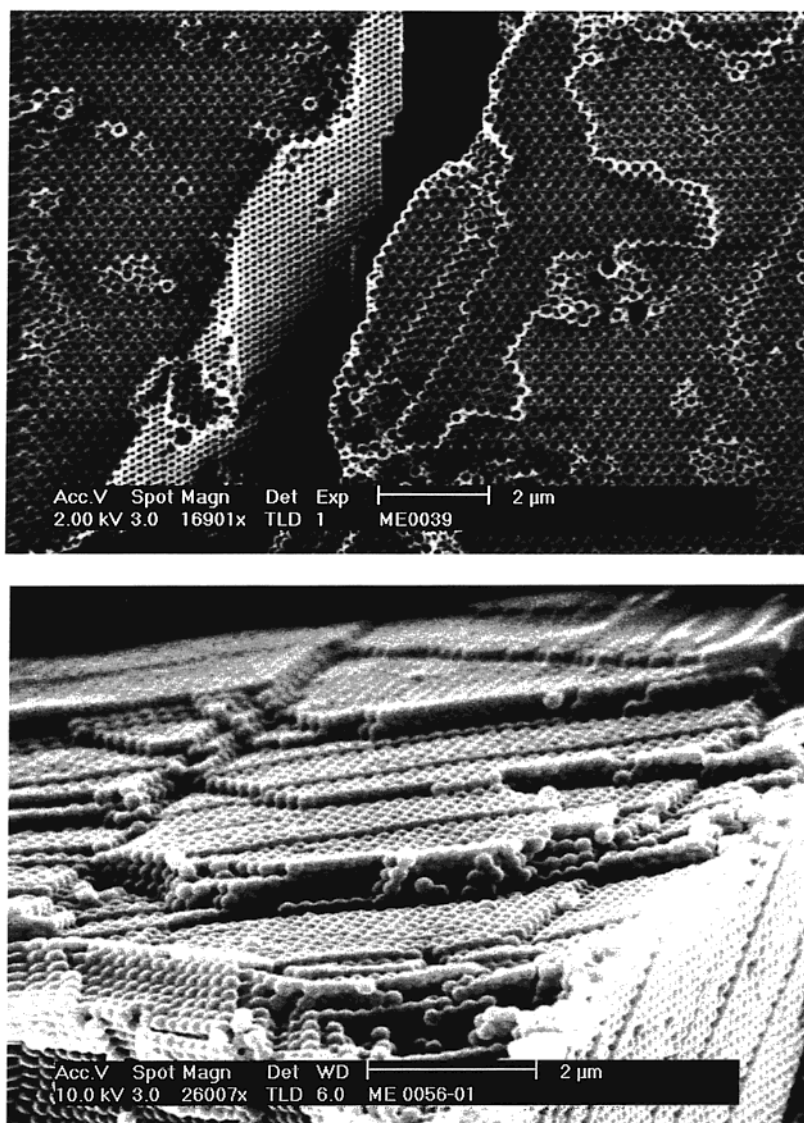


Figure 5. SEM images of C-tBMA-4 and C-tBMA/Et(5).

Table 2. Thermal Stability of Un-cross-linked and Cross-linked Photonic Structures: Comparison of T_g and the Fusing Temperature T_f

polymer	T_g (°C)	T_f (°C)
C-MMA-1	106	120–123
C-tBMA-4	109	133–137
C-MMA/Et(5)-2		>300
C-MMA/Et(2.5)		142–145
C-MMA/Et(1)	102	122–125
C-tBMA/Et(5)		>210

evaporation of remaining water between the beads. Next, the width of the cracks increase a second time slightly above T_g . This effect is probably due to a partial fusion of the polymer beads at their connecting points, which starts above T_g . The effect may be increased by a temperature gradient in the sample from the hotter glass plate to the cooler free surface. Finally, the beads fuse into a continuous film and the observed color disappears with both vertical and transmitted illumination (Figure 6). This final fusing temperature, T_f , is about 15–20 °C above T_g (120–123 °C for PMMA beads, 133–137 °C for PtBMA beads).

To increase the fusing temperature of the photonic structure further, we cross-linked the polymer within

the colloids (Table 2). At higher fractions of the cross-linker the fusing temperatures T_f increase tremendously compared to those of the homopolymer. A maximum effect was found for 5 mol % ethyleneglycolbismethacrylate in monomer solution. At lower concentrations T_f is only slightly increased. Either the cross-linker is not incorporated into the colloids or the surface tension is so strong that the soft, rubbery beads are forced to fuse despite some “penalty” in elastic energy. At higher concentrations of the cross-linker the size of beads becomes polydisperse and the crystallization is impeded. Therefore, 5 mol % of cross-linker seems to be the best choice for a synthesis of cross-linked monodisperse colloidal spheres.

The advantage of using cross-linked beads is best demonstrated by the heating experiment shown in Figure 6. The left side shows a thin photonic crystal film from un-cross-linked PMMA beads. Heating of this film to 150 °C for 3 min led to a fusion of an amorphous transparent PMMA film. The photonic crystal film from cross-linked PMMA (right side) showed a different behavior. After 1 h at 200 °C it was optically unchanged, except for an enlargement of the cracks due to loss of remaining water. Although the beads got rubbery above

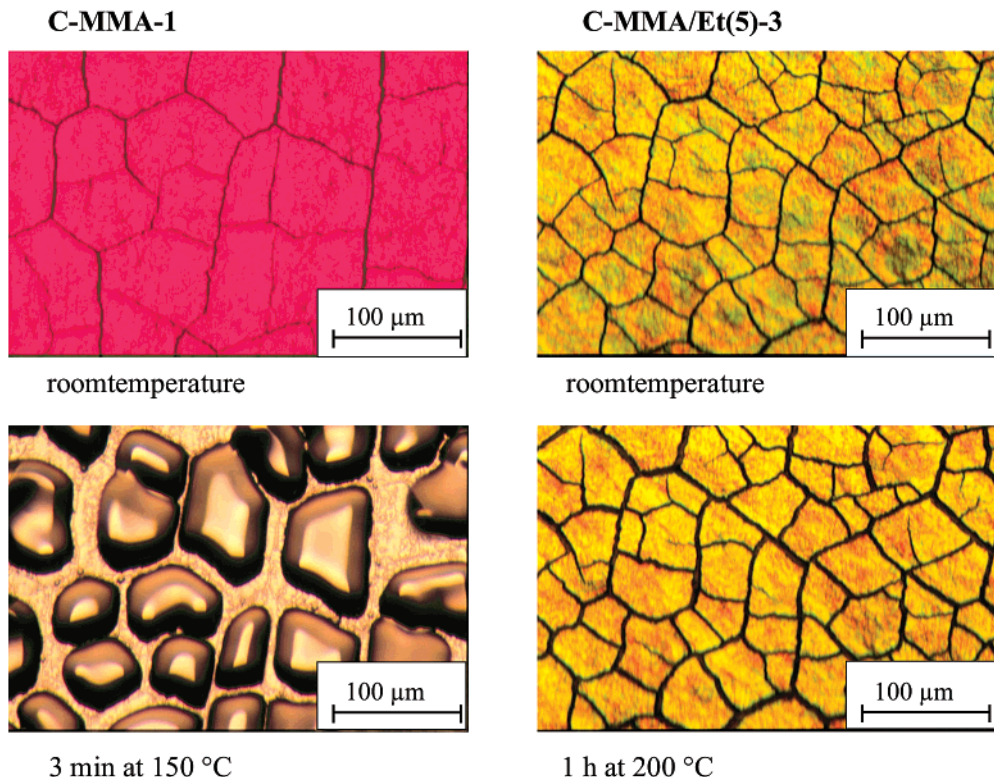


Figure 6. Thermal stability of un-cross-linked and cross-linked colloids from poly(methylmethacrylate); images were taken under a microscope; length of bars equals 100 μm .

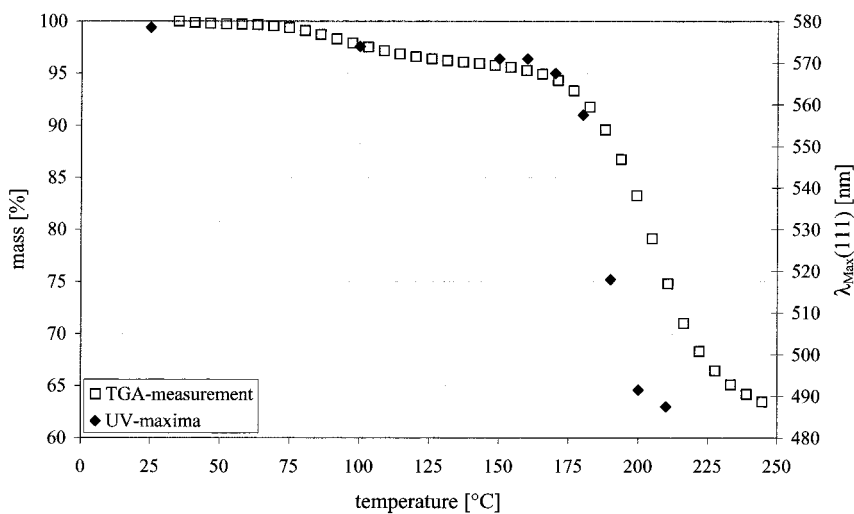


Figure 7. Comparison of thermogravimetric data with λ_{Max} for the annealing of **C-tBMA/Et(5)**.

T_g , they could not fuse. At the same time the beads got glued to each other very well, which increases their stability against redispersion in water (this will be discussed later in detail).

Thermogravimetric experiments show a complete burning off above 400 °C for both the un-cross-linked and the cross-linked PMMA. This issue is especially important for the removal of polymer latices by calcination after the infilling process.

Changing the Lattice Constants

Photonic films from cross-linked PtBMA showed a curious behavior. The Bragg reflection of **C-tBMA/Et(5)** shifted during annealing at 260 °C to the blue end of the visible electromagnetic spectrum (Figure 7).

According to eq 1, this could result either from a decrease of the effective refractive index due to porosity or from a decrease of the lattice constant due to shrinking beads. An interpretation of the result based only on the increase of porosity of the polymer beads can be ruled out. The change of the effective refractive index n_{eff} during a loss of 36% of bead material (thermogravimetry, Figure 7) is too small to explain the observed blue shift. The assumption of shrinking beads can, however, explain the results quantitatively. The theoretical weight loss due to a fission of the ester and the evaporation of isobutene is calculated to be 38% (thermogravimetry: 36%). Since PtBMA and poly(methacrylic acid) have comparable densities, a volume loss of about 40% is expected. This expectation corre-

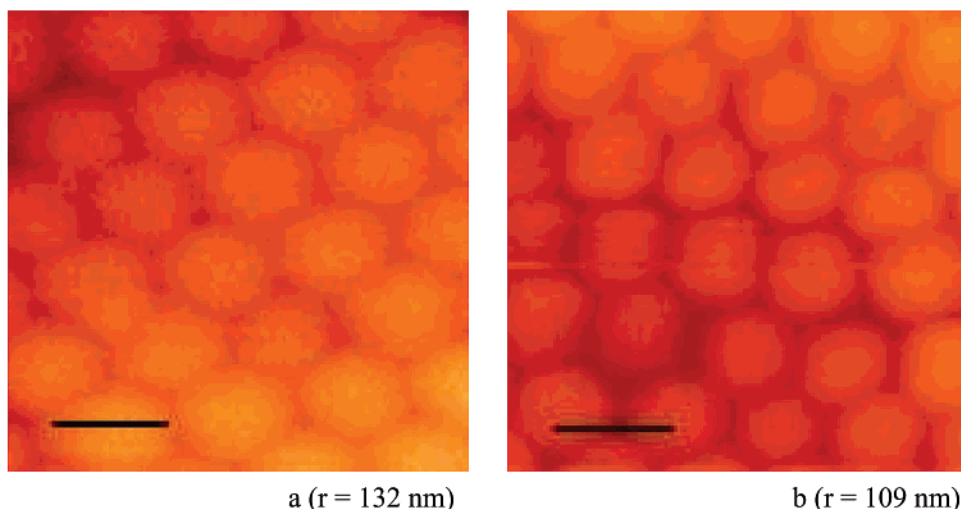


Figure 8. AFM images of **C-tBMA/Et(5)** before (a) and after (b) thermal treatment; image sizes, $1 \mu\text{m}^2$; length of bars equals 250 nm.

sponds exactly to the observation of a shift of the Bragg reflection (see Figure 7). At a volume loss of about 40% the radii of colloidal spheres are expected to decrease from 132 to 111 nm. These are just the radii needed to explain the blue shift (from $\lambda = 578 \text{ nm}$ to $\lambda = 488 \text{ nm}$). In addition, AFM photographs (Figure 8) of the crystal film before and after thermal treatment confirm this assumption of shrinking beads doubtlessly. Most interestingly, the volume loss (thermogravimetry) and the shift of the Bragg reflection occur at the same temperature (see Figure 7). Because of this result, the change of the color and the lattice parameter were secured as being generated by the fission of isobutene from the polymer. UV-vis measurements show, in addition, that the half bandwidth of the absorption increases during this process. Probably the lattice gets distorted because the photonic crystal film is glued to the rigid substrate (glass).

Surface Modification of Photonic Structures

If photonic structures from beads with highly charged or hydrophilic surfaces are desired, beads from polymethacrylates can be modified chemically by ester cleavage after crystallization in the dried film. The resulting crystal films cannot be prepared with self-assembly methods from solution because highly charged spheres interact over large distances. Therefore, crystallization happens with a large amount of water in the preformed crystal. During drying (necessary to have a high refractive index contrast) the resulting structure becomes more and more distorted and breaks finally into many tiny domains. Because *tert*-butyl esters are common protecting groups for acids, we initiated the ester cleavage from **C-tBMA/Et(5)** by acidic catalysis. If the acidic catalyst is soaked into the preformed photonic structure (this is rather easy as demonstrated by the work on replica formation¹⁷), the chemical ester cleavage should only happen at the surface in contrast to the thermal fission of isobutene. With acidic catalysis isobutene can be split off below 100 °C.

We worked out an acid-catalyzed cleavage in the liquid phase (liquid HCl). To realize this aim, the colloidal array needs to be stabilized first to prevent a

Table 3. Decrease of Contact Angle by Treatment of a Colloidal Film of C-tBMA/Et(5) with 3 M HCl

probe	contact angle (deg)
untreated	124
3 h at 80 °C	124
1 h at 50 °C with HCl	100
2 h at 50 °C with HCl	69

redispersion in water. For this purpose the dry films were heated close to T_g to allow partial fusion of the beads at their connecting points. This task is especially straightforward for the cross-linked colloids, which cannot fuse completely anyhow (see Figure 6). According to this, a colloidal crystal from cross-linked **C-tBMA/Et(5)** was heated to 80 °C for 3 h. To cleave isobutene, the crystal film was covered with a solution of 3 M hydrochloric acid and annealed at 50 °C for several hours (see Table 3). For a suitable detection of the surface modification, contact angle measurements were used. The fact that the measurement could be done proves the water stability of annealed films. We observed an increase in surface polarity with reaction time. As is shown in Table 3, advancing contact angles decreased from 124° to 69°.

Interestingly, IR measurements (transmission) of the chemically modified colloidal crystal showed no effects. This proves that the bulk material within the polymer beads is unaffected and that the ester cleavage is limited to the very surface of the beads. To ensure that the ester cleavage happens under these conditions, a polymer film with 15 wt % *para*-toluenesulfonic acid mixed in was spin-coated on silicon and annealed at 50 °C for 12 h. IR spectra (see Figure 9) left no doubt about the generation of acid groups with a shift of carbonyl band from 1724 to 1700 cm^{-1} and an appearance of a hydroxyl band at 3000 to 3500 cm^{-1} .

In summary, we succeeded in the preparation of photonic crystals from various polymethacrylates. A tremendous increase of the thermal stability was realized by cross-linking the polymer within the polymer beads. Thereby a larger temperature range (up to 200 °C for at least 1 h) became accessible, which can be used for infilling the artificial opal with high refractive inorganic materials and subsequent replica formation.

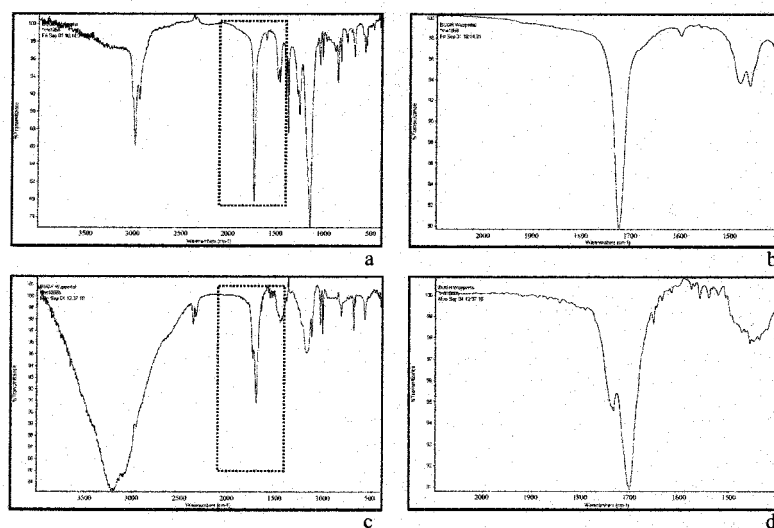


Figure 9. IR spectra of spin-coated poly(*tert*-butyl methacrylate) with 15 wt % *para*-toluenesulfonic acid before (a, b) and after heating (c, d) to 50 °C.

This is crucial for the creation of a full photonic band gap in the visible region from self-assembling processes.

In the case of cross-linked PtBMA we succeeded in the preparation of colloids that can be either thermally or chemically modified. Thermal modification led to shrinkable beads and a change in the optical properties of colloidal films. Chemically modified beads led to polymer opals from core–shell systems with hydrophilic polyelectrolytes in the shell.

Experimental Section

Reagents. The monomers used for polymerization were obtained from Merck or synthesized by a base-catalyzed esterification of methacrylic acid chloride and the corresponding alcohol. The initiator potassium peroxodisulfate was acquired from Aldrich and deionized water was obtained from a Milli-Q-system (Millipore).

Polymerization and Crystallization. The colloid particles from un-cross-linked PMMA were synthesized in a 10- or 250-mL flask with a nitrogen inlet and a magnetic stirrer. A flask was put in a 90 °C oil bath, charged with deionized water as described in Table 1, and flushed with nitrogen for 30 min. After the nitrogen flow was stopped, toluene and monomer were added in periods of several minutes to achieve temperature equilibrium. To start the polymerization, the potassium peroxodisulfate solution (10 wt %, annealed for 10 min at 90 °C under nitrogen) was added fast at once. The reaction solution was stirred at 1100–1250 rpm. The polymerization of tBMA was worked out without toluene. In the case of polymerizations with cross-linkers the monomer mixtures were prepared in advance and then added at once. During polymerization 0.5-mL fractions from reaction solution were isolated and spread on a glass slide and dried. The observed color gave roughly the diameter of the colloids. When the desired particle size was reached, the flask was opened (oxygen) to stop the polymerization and the remaining monomer was evaporated. The colloids were purified from large agglomerations by filtration through a standard paper filter. To get rid of smaller agglomerations and low molecular impurities, centrifugation followed. During centrifugation agglomerations sediment as white solid on the bottom of the centrifugation vial. The desired polymer beads sediment in an opalescent layer on top of the first layer. Low molecular impurities such as monomer, toluene, and initiator salt remained in the supernatant liquid. The first sedimenting layer was dumped and the liquid was exchanged with water in three to four centrifugation cycles.

For crystallization the colloids were suspended in water (about 10–30 wt % solution). The solution of about 5 μL was spread over an area of several square centimeters and dried at room temperature over days. To achieve controlled and high-humidity conditions (98%), the sample was placed in a chamber, which had been loaded with a crystallizing dish with concentrated KNO₃ solution in water.³¹ The higher the relative humidity, the longer the duration of crystallization. Domains of defect-free crystals increases up to 300 or 400 μm with longer crystallization periods (1 week).

Characterization was made via UV-vis spectroscopy and SEM or AFM microscopy.

To estimate the “melting” of the colloidal array, the crystal was heated in a hotstage (Linkam). The disappearance of the color caused by the Bragg reflection detected with the eye was defined as the fusing temperature because the polymer beads in the periodic structure of the array melted and flew to a polymer film.

The heating rate was chosen to be 4 °C/min to guarantee a full temperature exchange between the heat cell and the glass slide.

Used Instruments. IR spectra of the polymers were made with the FT-IR spectrometer Protege 460 ESP from Nicolet. Photonic structures were analyzed with a scanning spectrometer UV-2102 PC from Shimadzu. For the angle-dependent measurement the substrate was fixed vertically to a rotary plate and turned at the desired angle to the incident beam. Contact angle measurements were made on an OCA 20 from Data Physics. DSC characterization was made with DSC 7 from Perkin-Elmer. Thermogravimetric measurements of the polymers were worked out on a TG 50 from Mettler Toledo. Optical microscope observations were made with a SL 100 from Zeiss. Photographs were produced with the mirror reflection camera SC 35 from Olympus. Heating measurements were controlled with a digital control TMS 93.

Acknowledgment. We would like to thank the DFG (Schwerpunkt Photonische Kristalle) for funding this work. M. Brehmer (Univ. Mainz) is thanked for help with the AFM measurements. T. Maka (Univ. Wuppertal) and U. Jonas (MPI f. Polymerforschung) are thanked for help with the SEM measurements.

CM010375Z

(31) Kohlrausch, *Praktische Physik*, 3. Auflage; Teubner Verlag: Stuttgart, 1986; p 97.